Noncooperative Conflict Resolution *

Claire Tomlin, George J. Pappas and Shankar Sastry
Department of Electrical Engineering and Computer Sciences
University of California at Berkeley
Berkeley, CA 94720
{clairet,gpappas,sastry}@eecs.berkeley.edu

Abstract

Air Traffic Management Systems (ATMS) of the future allow for the possibility of *Free Flight*, in which aircraft choose their own optimal routes, altitude and speed. In a free flight environment, the trajectories of different aircraft may be conflicting, in which case aircraft may or may not cooperate in resolving the conflict. In this paper, noncooperative conflict resolution methods based on game theory are presented. Each aircraft models the actions of other aircraft as disturbances and tries to defend against the worst possible disturbance. This framework is applied in resolving conflicts between aircraft using speed and heading changes.

1 Introduction

Air transportation systems are faced with soaring demands for air travel. According to the Federal Aviation Administration (FAA), the annual air traffic rate in the U.S. is expected to grow by 3 to 5 percent annually for at least the next 15 years. The current National Airspace System (NAS) architecture and management will not be able to efficiently handle this increase because of several limiting factors including:

- **Inefficient airspace utilization:** Currently, the airspace is very rigidly structured and aircraft are forced to travel along predetermined jetways. This is clearly not optimal and disallows aircraft to fly directly to the destination and take advantage of favorable winds. This problem is particularly evident in transoceanic routes which are experiencing the greatest demand growth.
- **Increased Air Traffic Control (ATC) workload:** Separation among aircraft as well as vectoring aircraft in order to avoid weather hazards is performed centrally by ATC. The resulting centralized architecture places an enormous burden on controllers. In congested areas, such as close to urban airports, controllers simplify their heavy workload by routing aircraft on holding patterns.
- **Obsolete technology:** The computer technology used in most ATC centers is nearly 30 years old. Communication is restricted to congested voice communication between the aircraft

*Research supported by the Army Research Office under grants DAAH 04-95-1-0588 and DAAH 04-96-1-0341 and by NASA under grant NAG 2-1039.

and ATC. Navigation is performed by flying over fixed VHF Visual Omni-Directional Range (VOR) points. Developing weather storms are sometimes reported from aircraft to ATC.

In view of the above problems and in an effort to meet the challenges of the next century, the aviation community is working towards an innovative concept called *Free Flight* [1]. Free Flight allows pilots to choose their own routes, altitude and speed and essentially gives each aircraft the freedom to self-optimize. Aircraft flexibility will be restricted only in congested airspace in order to ensure separation among aircraft, or to prevent unauthorized entry of special use airspace (such as military airspace).

The economic benefits of Free Flight are immediate. Direct great circle routes, optimal altitudes, optimal avoidance of developing weather hazards and utilization of favorable winds will result in fuel burn and flight time operating cost savings. NASA studies [2] estimate that in a free flight scenario, user preferred trajectories could have resulted in annual potential savings of $1.28 billion in 1995 and could result in $1.47 billion savings in 2005[1].

Free Flight is potentially feasible because of enabling technologies such as Global Positioning Systems (GPS), Datalink communications, Automatic Dependence Surveillance-Broadcast (ADS-B), Traffic Alert and Collision Avoidance Systems (TCAS) [3] and powerful on-board computation. In addition, tools such as the Center-TRACON Automation System (CTAS) [4] will serve as decision support tools for ground controllers in an effort to reduce ATC workload and optimize capacity close to highly congested urban airports.

The above technological advances will also enable air traffic controllers to accommodate future air traffic growth by restructuring NAS towards a more decentralized architecture. The current system is extremely centralized with ATC assuming most of the workload. Sophisticated on-board equipment allow aircraft to share some of the workload, such as navigation, weather prediction and aircraft separation, with ground controllers. The resulting decentralized architecture clearly reduces the workload of ground controllers. Furthermore, such a distributed architecture is more fault tolerant to failures of centralized agencies.[2]

The road towards higher efficiency and flexibility must not compromise safety. Free Flight essentially removes a rigid structure which controllers normally use in order to predict and resolve conflicts. In order to improve the current standards of safety in an unstructured, Free Flight environment, automatic conflict detection and resolution algorithms are vital. Sophisticated algorithms which predict and automatically resolve conflicts would be used either on the ground or on-board, either as advisories or as part of the Flight Vehicle Management System (FVMS) of each aircraft. Current research endeavors along this direction include [5, 6, 7, 8, 9, 10, 11, 12, 13]

In [14, 15], a decentralized architecture for Air Traffic Management Systems (ATMS) is presented. In our design paradigm, aircraft are allowed to self-optimize in the spirit of Free Flight and coordinate with neighboring aircraft in order to resolve potential conflicts. Conflicts are classified as *cooperative* or *noncooperative*. In cooperative conflicts, aircraft exchange sensor and intent information in order to predict and resolve the conflict. In noncooperative conflicts, aircraft do not collaborate in resolving the conflict. Such a situation arises, for example, when a fully equipped commercial aircraft is in conflict with a general aviation aircraft which is technologically challenged (ie. one that is unequipped with modern communication and navigation devices). It can also occur in the case of communication malfunctions. Clearly, in a noncooperative scenario, each aircraft

[1]Using forecasted air traffic demand for 2005

[2]Such as the power failure at the Oakland Center in 1995.

does not know of the intent of the other aircraft.

In this paper, we focus on noncooperative conflict resolution. A natural framework for problems in which many aircraft have conflicting objectives is game theory [16, 17, 18]. In this framework, each aircraft treats every other aircraft as a disturbance. Assuming a saddle solution to the game exists, the aircraft chooses an optimal policy assuming the worst possible disturbance or actions of the other aircraft. If the optimal policy is safe for worst disturbance then it will also be safe for any disturbance or actions of the noncooperating aircraft. Given a saddle solution, the safe set of initial conditions is calculated as well as the space of safe controls. Secondary objectives such as efficiency and passenger comfort can be accommodated by solving an optimal control problem in the set of controls which guarantee safety. In addition, the solutions of the games are abstracted in the form of *protocols* among the aircraft. Our approach treats conflicts on a pairwise basis.

The organization of this paper is as follows. In Section 2, a conflict resolution strategy is described, and in Section 3 relative kinematic aircraft models are derived. Section 4 describes the game theoretic approach to noncooperative conflict resolution and Section 5 discusses issues for further research.

2 Conflict Resolution Strategy

In Free Flight, aircraft wish to traverse different trajectories which have been designed in an optimal fashion according to the goals of each aircraft [19, 20]. Very frequently, however, the trajectories of two or more aircraft may be conflicting. A conflict resolution strategy has to choose a proper balance between centralized and decentralized authority. Central agencies, in general, are concerned with global issues while individual agents are concerned with local problems. Conflict among aircraft is essentially a local problem and it seems natural to address this problem in a decentralized fashion. *We therefore propose a conflict resolution strategy in which conflicts are resolved locally with minimal ATC intervention.* This will clearly reduce ATC workload, to focus on more global issues such as traffic flow management.

Figure 1 outlines such a conflict resolution strategy. Initially, aircraft are assumed to be in *Free Flight* mode in which the aircraft is tracking a self-optimal trajectory. Each aircraft is surrounded by two virtual *hockey pucks*, the *Protected Zone* and the *Alert Zone*, shown in Figure 2. A conflict between two aircraft occurs whenever the protected zones of the aircraft overlap. The radius and the height of the en-route protected zone is currently 5 nautical miles and 2,000 ft respectively. It is rather clear that the success of Free Flight will depend on the relative time that each aircraft is allowed to optimize its own goals. Improved navigation and surveillance allow for the reduction of the protected zone to 3 nautical miles and 1,000 ft. Informal studies [1] show that given the same aircraft population and routes of flight such a reduction of the protected zone will result in a decrease of conflicts by almost 70% and would clearly increase airspace utilization.[3] This will allow aircraft to stay on their nominal, optimized trajectories for as long as possible. The size of the alert zone depends on various factors including airspeed, altitude, accuracy of sensing equipment, traffic situation, aircraft performance and average human and system response times. The Alert Zone should be large enough to allow a comfortable system response but also small enough in order to avoid unnecessary conflicts.

Once the alert zone of an aircraft is violated by another aircraft, an attempt is made to *establish*

[3]This study does not reflect the possible increase in controller workload by compressing traffic

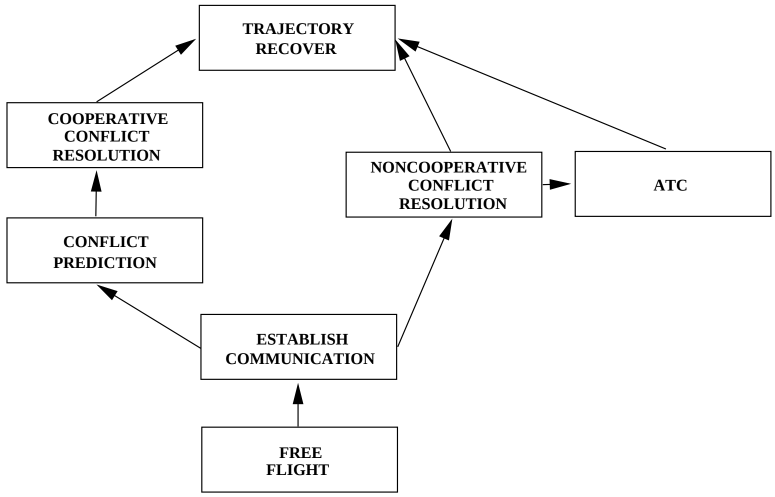

Figure 1: Conflict Resolution Architecture

communication. The purpose of the communication is to transmit and receive accurate position, heading, velocity information as well as short term intent of each aircraft. This is feasible with technologies such as ADS-B. In addition, if the communication is successful, aircraft are assumed to cooperate in order to resolve a potential conflict.

In the case of successful communication, the gathered data are transmitted to the *Conflict Prediction* module where it is determined whether or not a conflict will occur in the near future. Conflict prediction could be spatial, temporal or probabilistic. Spatial and temporal approaches, such as [7, 8, 13], calculate the four dimensional coordinates of a possible conflict. Probabilistic approaches, such as [5, 6], assume stochastic uncertainty in the measured information and determine the probability of collision. In either case, if there is no (or low-probability) conflict, then aircraft return to their Free Flight mode. If a conflict is predicted (or has very high probability), aircraft enter the *Cooperative Conflict Resolution* mode. In this mode, aircraft perform predetermined coordinated maneuvers which are guaranteed to be safe by construction. Such an approach is proposed in [13]. These maneuvers are a combination of a verified communication protocol as well as control laws. The class of maneuvers constructed to resolve conflicts must be rich enough to cover most possible conflict scenarios.

In many cases, however, communication between aircraft may not be established. This situation occurs when one of the aircraft, such as general aviation aircraft, may not be equipped with sophisticated avionics or when there is a communication malfunction. In this case, on-board sensing is still able to provide accurate state estimates about the intruding aircraft, possibly with a larger uncertainty. The intent or actions of the other aircraft, however, cannot be known without communication. In this case, we propose the use of *Noncooperative Conflict Resolution*, which is the subject of this paper. In this framework, each aircraft assumes the worst possible action or intent of the intruding aircraft and calculates an optimal policy in order to defend against the worst possible action. If the policy is safe for the worst action of the intruding aircraft then it is safe for any action of the intruding aircraft.

The natural framework to perform noncooperative conflict resolution is game theory. Aircraft are treated as players in a zero-sum noncooperative dynamic game. Each player is aware only of the possible actions of the other agents. These actions are modeled as disturbances, assumed to lie

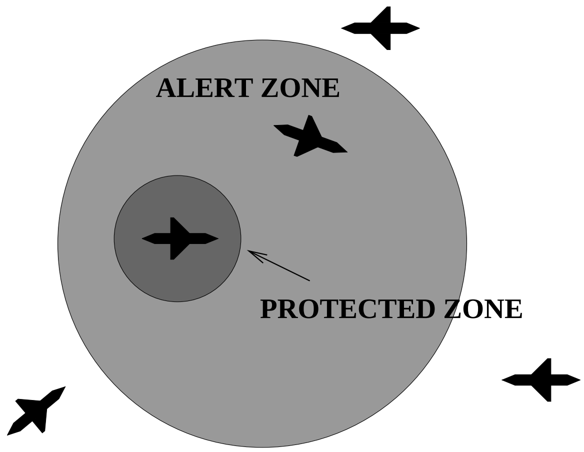

Figure 2: Aircraft Zones

within a known set but with their particular values unknown and uncontrolled. Each aircraft solves the game considering the worst possible disturbance. An aircraft is considered to have lost the game if the other aircraft penetrates its protected zone. Using this criterion, the safe set of states and the space of safe controls for each aircraft may be calculated.

If the saddle solution to the game does not exist or is unsafe, then the aircraft may ask for ATC intervention in order to resolve the conflict. Once the conflict is resolved either cooperatively or noncooperatively, aircraft enter the *Trajectory Recover* mode, where aircraft reconverge to the original, optimal trajectory. The aircraft then returns to the Free Flight mode.

3 Modeling

Because conflicts between agents depend on the relative position and velocity of the agents, it is useful in the following analysis to derive *relative* kinematic models, describing the motion of each aircraft in the system with respect to the other aircraft. For example, to study pairwise conflict between the trajectories of two aircraft, aircraft 1 and aircraft 2, a relative model with its origin centered on aircraft 1 is used.

The configuration of an individual agent is described by an element of a Lie group G. The Lie group G will typically be either the group of rigid motions in $\mathbb{R}^2$ or $\mathbb{R}^3$, called $SE(2)$ or $SE(3)$ respectively. In planar situations, in which aircraft are flying at the same altitude, $SE(2)$ will be used.

Following the example described above, let $g_1 \in G$ denote the configuration of aircraft 1, and let $g_2 \in G$ denote the configuration of aircraft 2. The trajectories of both aircraft are kinematically modeled as left invariant vector fields on G. Therefore

$$\dot{g}_1 = g_1 X_1 \tag{1}$$
$$\dot{g}_2 = g_2 X_2 \tag{2}$$

where $X_1, X_2 \in \mathcal{G}$, the Lie algebra associated with the Lie group G.

A coordinate change is performed to place the identity element of the Lie group G on aircraft 1.

Thus, let $g_r \in G$ denote the relative configuration of aircraft 2 with respect to aircraft 1. Then

$$g_2 = g_1 g_r \Rightarrow g_r = g_1^{-1} g_2 \tag{3}$$

Differentiation yields the dynamics of the relative configuration,

$$\dot{g}_r = g_r X_2 - X_1 g_r \tag{4}$$

Note that the vector field which describes the evolution of g_r is neither left nor right invariant. However,

$$\begin{aligned} \dot{g}_r &= g_r X_2 - X_1 g_r \\ &= g_r [X_2 - Ad_{g_r^{-1}} X_1] \end{aligned} \tag{5}$$

where $Ad_{g_r^{-1}} X_1 = g_r^{-1} X_1 g_r \in \mathcal{G}$.

Consider the Lie group $SE(2)$ and its associated Lie algebra $se(2)$. A coordinate chart for $SE(2)$ is given by x, y, ϕ representing the planar position and orientation of a rigid body. In this coordinate chart, the relative configuration g_r is given in homogeneous coordinates by

$$g_r = \begin{bmatrix} \cos\phi_r & -\sin\phi_r & x_r \\ \sin\phi_r & \cos\phi_r & y_r \\ 0 & 0 & 1 \end{bmatrix} \tag{6}$$

where x_r, y_r represent the relative position of aircraft 2 with respect to aircraft 1 and ϕ_r is the relative orientation. The Lie algebra elements $X_1, X_2 \in se(2)$ are represented as matrices in $\mathbb{R}^{3\times 3}$ of the form

$$X_1 = \begin{bmatrix} 0 & -\omega_1 & v_1 \\ \omega_1 & 0 & 0 \\ 0 & 0 & 0 \end{bmatrix} \qquad X_2 = \begin{bmatrix} 0 & -\omega_2 & v_2 \\ \omega_2 & 0 & 0 \\ 0 & 0 & 0 \end{bmatrix} \tag{7}$$

where v_i, ω_i represent the translational and rotational velocities. Inserting equations (6) and (7) in equation (4) results in the following model

$$\begin{aligned} \dot{x}_r &= -v_1 + v_2 \cos\phi_r + \omega_1 y_r \\ \dot{y}_r &= v_2 \sin\phi_r - \omega_1 x_r \\ \dot{\phi}_r &= \omega_2 - \omega_1 \end{aligned} \tag{8}$$

illustrated in Figure 3.

Now consider the Euclidean group $SE(3)$ along with its associated Lie algebra $se(3)$. A coordinate chart for $SE(3)$ is given by $x, y, z, \phi, \theta, \psi$ representing the planar position and orientation. The orientation is parameterized using the yaw-pitch-roll chart where ψ is the yaw, θ is the pitch and ϕ is the roll. In this coordinate chart, the relative configuration g_r is given in homogeneous coordinates by

$$g_r = \begin{bmatrix} C\psi_r C\theta_r & C\psi_r S\theta_r S\phi_r - S\psi_r C\phi_r & C\psi_r S\theta_r C\phi_r + S\phi_r S\psi_r & x_r \\ S\psi_r C\theta_r & S\psi_r S\theta_r S\phi_r + C\psi_r C\phi_r & S\psi_r S\theta_r C\phi_r - S\phi_r C\psi_r & y_r \\ -S\theta_r & C\theta_r S\phi_r & C\theta_r C\phi_r & z_r \\ 0 & 0 & 0 & 1 \end{bmatrix} \tag{9}$$

where x_r, y_r, z_r represent the relative position of aircraft 1 in the coordinate system which is attached to aircraft 1 and ϕ_r, θ_r, ψ_r parameterize the relative orientation. In equation (9), the notation $S\alpha$

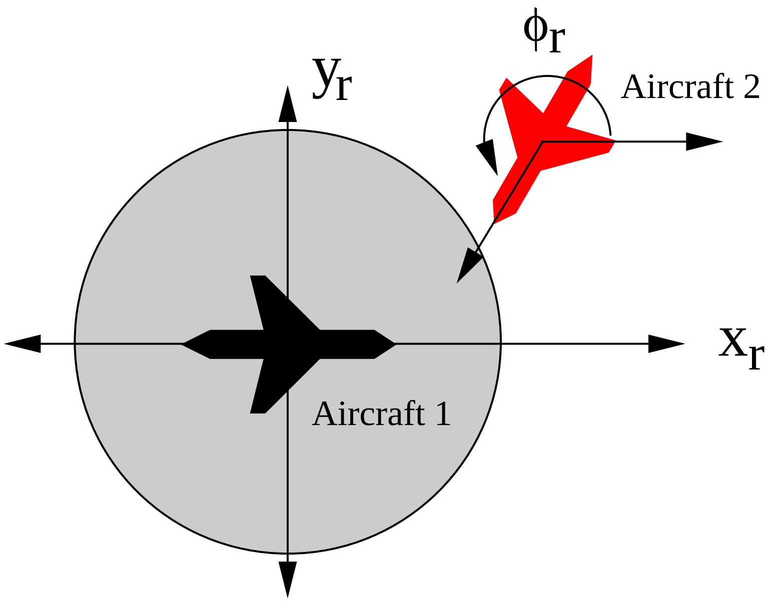

Figure 3: The relative configuration model

stands for the sine of the angle α and $C\alpha$ for the cosine. The Lie algebra elements $X_1, X_2 \in se(3)$ are of the following form

$$X_1 = \begin{bmatrix} 0 & -\omega_3^1 & \omega_2^1 & v_1 \\ \omega_3^1 & 0 & -\omega_1^1 & 0 \\ -\omega_2^1 & \omega_1^1 & 0 & 0 \\ 0 & 0 & 0 & 0 \end{bmatrix} \qquad X_2 = \begin{bmatrix} 0 & -\omega_3^2 & \omega_2^2 & v_2 \\ \omega_3^2 & 0 & -\omega_1^2 & 0 \\ -\omega_2^2 & \omega_1^2 & 0 & 0 \\ 0 & 0 & 0 & 0 \end{bmatrix} \tag{10}$$

where $v_i, \omega_1^i, \omega_2^i, \omega_3^i$ represent the translational and rotational velocities of aircraft i.. Inserting equations (9) and (10) in equation (4) results in the following model

$$\begin{aligned}
\dot{x}_r &= -v_0 - \omega_3^1 y_r - \omega_2^1 z_r + v_1 \cos\psi_r \cos\theta_r \\
\dot{y}_r &= -\omega_3^1 x_r + \omega_1^1 z_r + v_1 \sin\psi_r \cos\theta_r \\
\dot{z}_r &= \omega_2^1 x_r - \omega_1^1 y_r - v_1 \sin\theta_r \\
\dot{\theta}_r &= -\omega_2^1 C\psi_r + \omega_2^2 C\phi_r + \omega_1^1 S\psi_r - \omega_3^2 S\phi_r \\
\dot{\psi}_r &= -\omega_3^1 + \frac{1}{C\theta_r}[-\omega_2^1 S\psi_r S\theta_r + \omega_2^2 S\phi_r + \omega_3^2 C\phi_r - \omega_1^1 C\psi_r S\theta_r] \\
\dot{\phi}_r &= \omega_1^2 + \frac{1}{C\theta_r}[\omega_3^2 C\phi_r S\theta_r - \omega_2^1 S\psi_r - \omega_1^1 C\psi_r + \omega_2^2 S\phi_r S\theta_r]
\end{aligned} \tag{11}$$

Notice that equations (11) are ill posed when $\theta_r = \pm\frac{\pi}{2}$ as expected from the singularity of the yaw-pitch-roll parameterization of $SE(3)$.

4 Noncooperative Conflict Resolution

4.1 Design philosophy: game theoretic approach

We step back from the specific kinematic model described in the previous section to describe our noncooperative conflict resolution design philosophy on the general relative configuration model:

$$\dot{x} = f(x, u, d, t) \qquad x(t_0) = x_0 \tag{12}$$

where $x \in \mathbb{R}^n$ describes the relative configuration of one of the aircraft with respect to the other, $u \in \mathcal{U}$ is the control input of one agent, and $d \in \mathcal{D}$ is the control of the other agent.

Our design philosophy is as follows: Suppose that the two aircraft are conflict-prone, and they cannot cooperate to resolve conflict due to any one of the reasons mentioned in the previous section. Then the safest possible strategy of each aircraft is to fly a trajectory which guarantees that the minimum allowable separation with the other aircraft is maintained, *regardless* of the actions of the other aircraft. Since the intent of each aircraft is unknown to the other, then this strategy must be safe for the *worst possible actions* of the other aircraft. We solve this problem by using the framework of two person zero sum dynamical games (specifically pursuit-evasion games) to characterize the *safe sets* of states and control inputs for each aircraft, given the set of possible actions of the other aircraft. Efficient trajectories, such as ones which minimize the deviation from the aircraft's original route, may be chosen from these safe sets.

We call the aircraft at the origin of the relative frame the evader, and the other aircraft the pursuer. The game evolves over the fixed time interval $[t_0,\ t_f]$, where t_f is given by

$$t_f = \inf\{t \in \mathbb{R}^+ : (x(t), t) \in T\} \tag{13}$$

Here T is the *target set*, a closed subset of $\mathbb{R}^n \times \mathbb{R}^+$ which describes those states for which the game is lost by the evader. We assume that the boundary ∂T of T may be described by the function $l(x, t) = 0$. The game is called zero sum, because one player (evader) seeks to maximize and the other (pursuer) to minimize the single cost function

$$J(x_0, u, d) = \phi(x(t_f), t_f) + \int_{t_0}^{t_f} L(x, u, d, t)dt \tag{14}$$

where $L(x, u, d, t)$ is the running cost and $\phi(x(t_f), t_f)$ is the cost at the final time. We also assume that the game has *perfect information*, meaning that both players have access to the full state $x(t)$. We have noted in the previous section that this assumption is fairly reasonable: although the aircraft do not communicate with each other to determine each other's intent and resolution strategy, the state of the aircraft may be determined by the other through sensor input. The error in this sensor information may be incorporated into the problem as ranges on the actual value.

The problem is now to minimize over u and maximize over d the cost function (14) subject to the dynamic constraint (12). We form the Hamiltonian

$$H(x, u, d, p, t) = L(x, u, d, t) + p^T f(x, u, d, t) \tag{15}$$

where $p(t) \in \mathbb{R}^n$ is the Lagrange multiplier for the dynamic constraint, or the costate of the system. The game is said to have a saddle point solution (u^*, d^*) if

$$\min_u \max_d H(x, u, d, p, t) = \max_d \min_u H(x, u, d, p, t) \tag{16}$$

and this saddle solution is calculated as

$$u^*(t) = \arg\min_u \max_d H(x,u,d,p,t), \quad d^*(t) = \arg\max_d \min_u H(x,u,d,p,t) \tag{17}$$

The resulting optimal Hamiltonian is denoted by $H^*(x,p,t)$. The equations for the evolution of the state and costate along the optimal Hamiltonian are given by the Hamilton-Jacobi equations:

$$\begin{aligned} \dot{x} &= \frac{\partial H^*}{\partial p}(x,p,t) \\ \dot{p} &= -\frac{\partial H^*}{\partial x}^T(x,p,t) \end{aligned} \tag{18}$$

with $x(t_0) = x_0$ and $p^T(t_f) = \frac{\partial}{\partial x}\phi(x(t_f), t_f)$. The solution of these equations provides the saddle solution, the *best* control action of the evader for the *worst* disturbance of the pursuer for the given initial condition of the kinematic model. The set of *safe initial conditions* is defined as

$$V = \{x_0 \in \mathbb{R}^n | J(x_0, u, d^*) \geq C\} \tag{19}$$

where C encodes the size of the protected zone around each aircraft. For each $x_0 \in V$,

$$\mathcal{U}(x_0) = \{u \in \mathcal{U} | J_s(x_0, u, d^*) \geq C\} \tag{20}$$

is the set of *safe control policies* which guarantees safety from relative configuration x_0. Since all $u \in \mathcal{U}(x_0)$ guarantee safety from x_0, it is advantageous to find the control policy $u \in \mathcal{U}(x_0)$ that minimizes deviation from the nominal trajectory, which is encoded by a second cost function J_2, usually a quadratic function of the tracking error. To do this, we solve the optimal control problem which is *nested inside* the differential game calculation:

$$\min_{u \in \mathcal{U}(x_0)} J_2 \tag{21}$$

subject to the original differential equations (1), (2) which describe the aircraft motion in absolute coordinates. Additional system requirements, such as *passenger comfort*, can now be incorporated by extending the above nested chain of games and optimal control problems [21].

In order to solve the dynamical game above (for safety), we pose the problem as referred to in Başar and Olsder [16] as one of "capturability". In these problems the Lagrangian $L(x,u,d,t) = 0$, since there is no running cost, we are interested only in whether or not the pursuer ends up in the target set T. We assume that the system is time invariant, so that the system kinematics and the target set do not depend on time. T is defined to be the protected zone of the evader. Thus the cost function is simply

$$J = \begin{cases} -1 \text{ if } x(t) \in T \text{ for some } t, \ 0 \leq t < \infty \\ +1 \text{ otherwise} \end{cases} \tag{22}$$

To solve this qualitative game, we first characterize the *unsafe* portion of ∂T, defined as those states along this boundary for which the pursuer can enter T, regardless of the control u applied by the evader. We denote the outward pointing normal to T as

$$\nu = \frac{\partial l}{\partial x}^T(x(t_f)) \tag{23}$$

as in Figure 4. The unsafe part of ∂T is the $x(t_f)$ along this boundary for which there is some

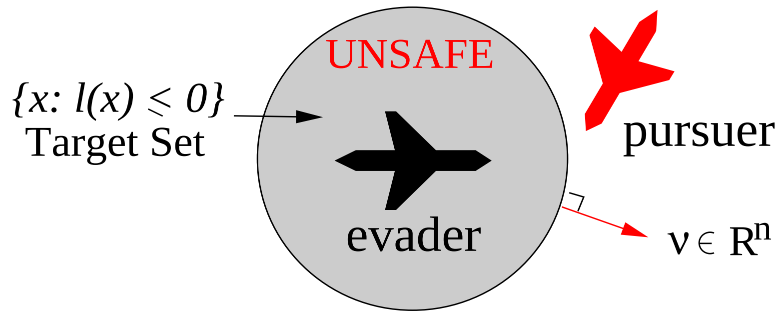

Figure 4: The evader and pursuer, with Target set and its outward pointing normal ν

disturbance $d \in \mathcal{D}$ such that $f(x(t_f), u^*, d, t_f)$ points into T; the safe part is the $x(t_f)$ for which there is some input $u \in \mathcal{U}$ such that $f(x(t_f), u, d^*, t_f)$ points outward from T:

$$\begin{array}{ll} \text{Safe} & \{x(t_f) : \exists u \forall d \quad \nu^T f(x(t_f), u, d, t_f) \geq 0\} \\ \text{Unsafe} & \{x(t_f) : \forall u \exists d \quad \nu^T f(x(t_f), u, d, t_f) < 0\} \end{array} \tag{24}$$

Since the Lagrangian is zero, the Hamiltonian is simply

$$H(x, u, d, p, t) = p^T f(x, u, d, t) \tag{25}$$

where $p^T(t_f) = \nu$. On the boundary ∂T, the optimal Hamiltonian is

$$H^*(x, p, t_f) = \sup_{u \in \mathcal{U}} \inf_{d \in \mathcal{D}} H(x, u, d, p, t_f) \tag{26}$$

If $H^*(x, p, t_f) \geq 0$, the evader can flee, and if $H^*(x, p, t_f) < 0$ the pursuer catches the evader. With this characterization of the safe and unsafe portions of ∂T, we can propagate the boundaries of the safe set (those points for which $l(x, t) = 0$ and $H^*(x, p, t_f) = 0$) backwards in time, using the Hamilton-Jacobi equations (18), to determine the safe and unsafe sets over the state space $\mathbb{R}^n$ (see Figure 5).

With the safe set calculated, we can solve for the most efficient trajectory within the safe set of initial conditions and control inputs. The problem can be posed as an optimal control problem in which we minimize the tracking error, subject to the state and input constraints for safety. This is an analytically difficult problem, and our approximate solutions will be presented in the final version of this paper.

4.2 Constant Altitude Conflict Resolution

In this section, we apply this general framework to conflicts which occur among aircraft at the same altitude. These conflicts are resolved either by speed variations or by path deviations. We therefore use the planar $SE(2)$ model (8).

We first fix the linear velocities v_1, v_2, and let the aircraft avoid conflict solely by using their angular velocities ω_1, ω_2. Using the method described above, we can calculate the safe sets of states for this relative model as follows. The target set T is the protected zone of the pursuer, and its boundary ∂T is a cylinder in the (x_r, y_r, ϕ_r) space with a radius of 5 miles. The safe and unsafe portions of ∂T are calculated using equations (24). The saddle solution (ω_2^*, ω_1^*) is then determined for each point

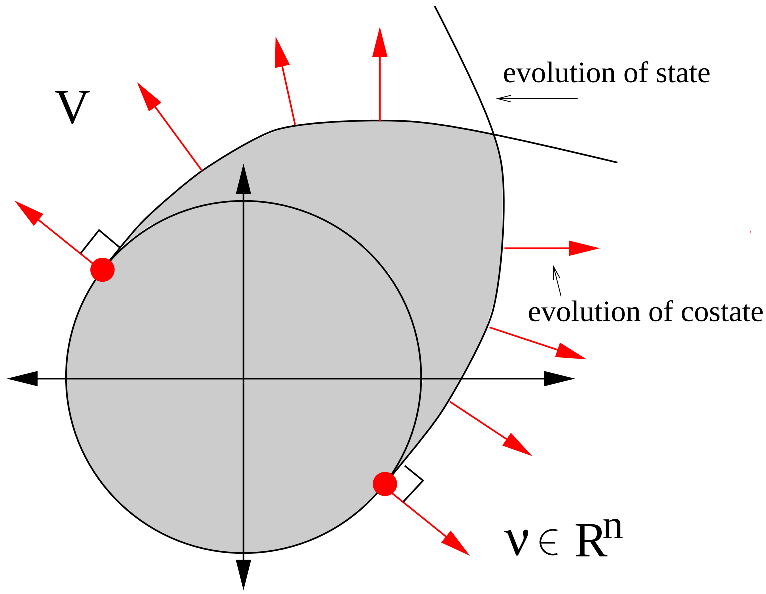

Figure 5: The unsafe set of states (shaded) and its complement (the safe set V)

on the boundary of the safe portion on ∂T, and the model equations (8) are integrated backwards in time from this boundary, using (u^*, d^*) as the control and disturbance inputs in these equations. The results of this calculation are shown in Figures 6 and 7 for equal pursuer and evader linear velocities ($v_1 = v_2 = 1.5$), for a pursuer angular velocity of $\omega_1 \in [0, 0.1]$, and for an evader angular velocity of $\omega_2 = 0.1$. Outside of the boundary of the unsafe set, any control input may be applied by the evader, whereas on the boundary, the only input which may be applied to ensure safety is u^*. If the evader is inside the unsafe set, it will eventually end up in the target set regardless of its actions.

We note that the computation of these unsafe sets is in general difficult at so-called "singular" points. For certain inputs, the surfaces shown in Figures 6 and 7 do not intersect, or the intersection of these surfaces contain holes. Even if the two surfaces intersect, it is not clear that the line of intersection maintains property that u^* is the unique safe input. Since at this point we have only been able to classify these properties geometrically on a case by case basis, it has been impossible for us to use this method on models of dimension greater than three. Fortunately for the example in this paper, we have been able to make the following simplifying assumption which makes the calculation of these unsafe sets easier.

The assumption in this solution is that the worst case action of the pursuing aircraft corresponds to a "dogfight" scenario, in which the pursuer constantly changes heading and chases the evader. This assumption is (happily) too conservative for civilian flight: for the most part, civilian aircraft travel in straight lines with few heading changes. When heading changes are made, they are generally 5° to 30° changes. We therefore consider two special cases of the full $SE(2)$ model (8): (i) the aircraft are restricted to straight line motion and so conflicts are resolved by altering velocity variations; and (ii) the aircraft are restricted to constant velocity and straight line motion, except at discrete instants of time at which they can make instantaneous heading changes of 5° to 30°.

In this paper, we make the additional simplifying assumption that in case (ii), discrete heading changes only occur by the evader in attempting to avoid conflict: the pursuer remains on its

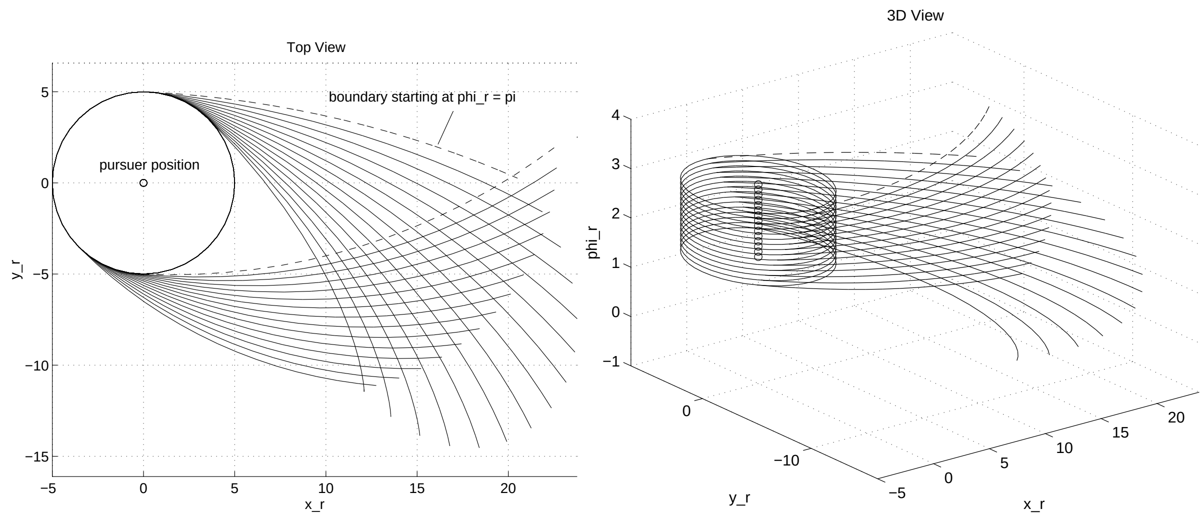

Figure 6: The top and 3D views of the Target set T around the pursuer and the unsafe set of configurations of the evader with respect to the pursuer.

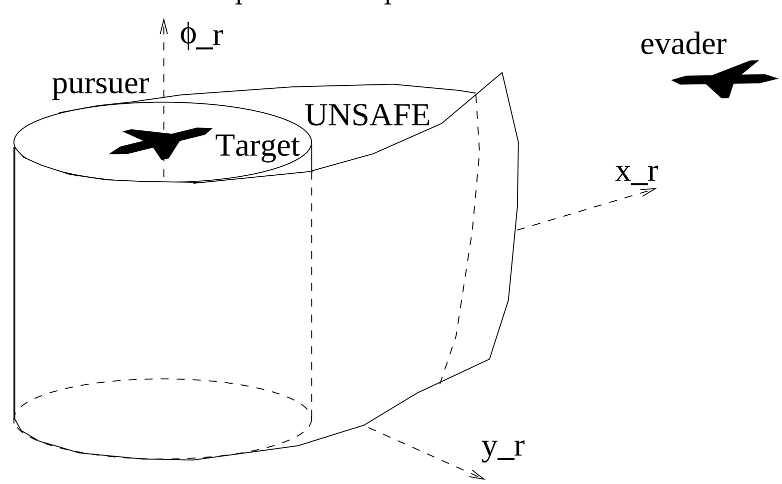

Figure 7: Same as above, showing the pursuer and evader. The target set T is simply the protected zone of the pursuer.

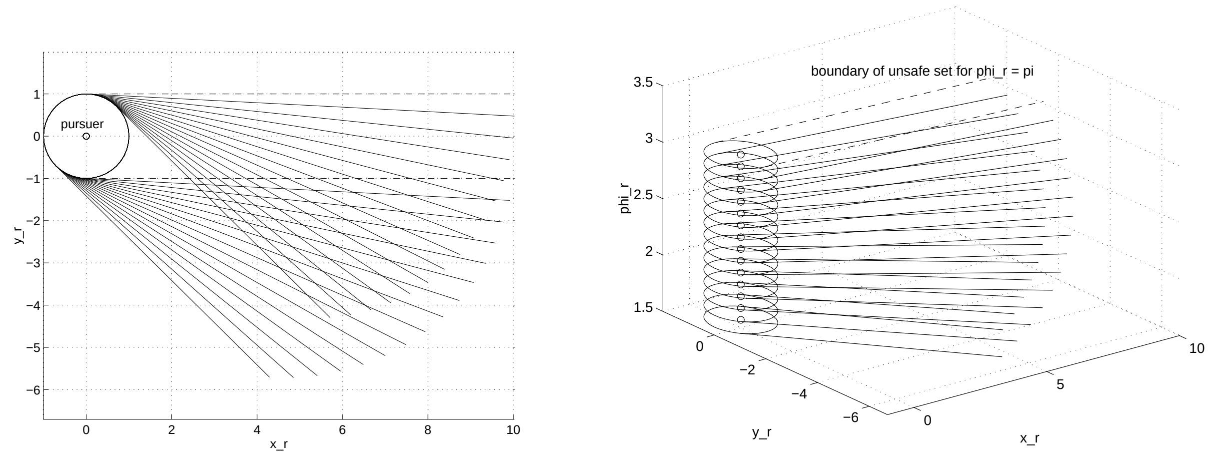

Figure 8: The top and 3D views of the target set T around the pursuer and the unsafe sets for the evader for various headings ϕ_r; the unsafe set for $\phi_r = \pi$ is shown with its boundaries as dotted lines for emphasis. The sets boundaries extend backwards infinitely.

original course. The notion of "noncooperative" therefore means that the pursuer does not take part in the resolution maneuver. The model becomes

$$\begin{aligned} \dot{x}_r &= -v_1 + v_2 \cos \phi_r \\ \dot{y}_r &= v_2 \sin \phi_r \\ \dot{\phi}_r &= \Delta_2 \delta(t - t_0) \end{aligned} \tag{27}$$

where Δ_2 is the magnitude of the heading change and t_0 is the instant at which the heading change occurs. Figure 8 illustrates the unsafe sets of the evader relative to the pursuer for $\Delta_2 = 0$ and $\pi/2 \leq \phi_r \leq \pi$. The unsafe sets are simple: they have straight line boundaries which extend infinitely backwards from the target set, and their intersection with the target set depends on ϕ_r.

4.2.1 Resolution by Linear Velocity

We first consider case (i), in which $\Delta_2 = 0$, v_1 is the disturbance input and v_2 is the control input. The input and disturbance lie in closed subsets of the positive real line,

$$v_2 \in \mathcal{U} = [\underline{v}_2, \overline{v}_2] \subset \mathbb{R} \tag{28}$$

$$v_1 \in \mathcal{D} = [\underline{v}_1, \overline{v}_1] \subset \mathbb{R} \tag{29}$$

with $\underline{v}_2 > 0$ and $\underline{v}_1 > 0$. Assuming that v_1 and v_2 are constant (a valid assumption since they are constant at their maximum or minimum bounds in the saddle solution), equations (27) can be integrated:

$$\begin{aligned} x_r(t) &= x_r(0) + (-v_0 + v_1 \cos \phi_r)t \\ y_r(t) &= y_r(0) + (v_1 \sin \phi_r)t \\ \phi_r(t) &= \phi_r(0) \end{aligned} \tag{30}$$

For this case, the saddle solution (u^*, d^*) can be calculated analytically (see [13]) and is:

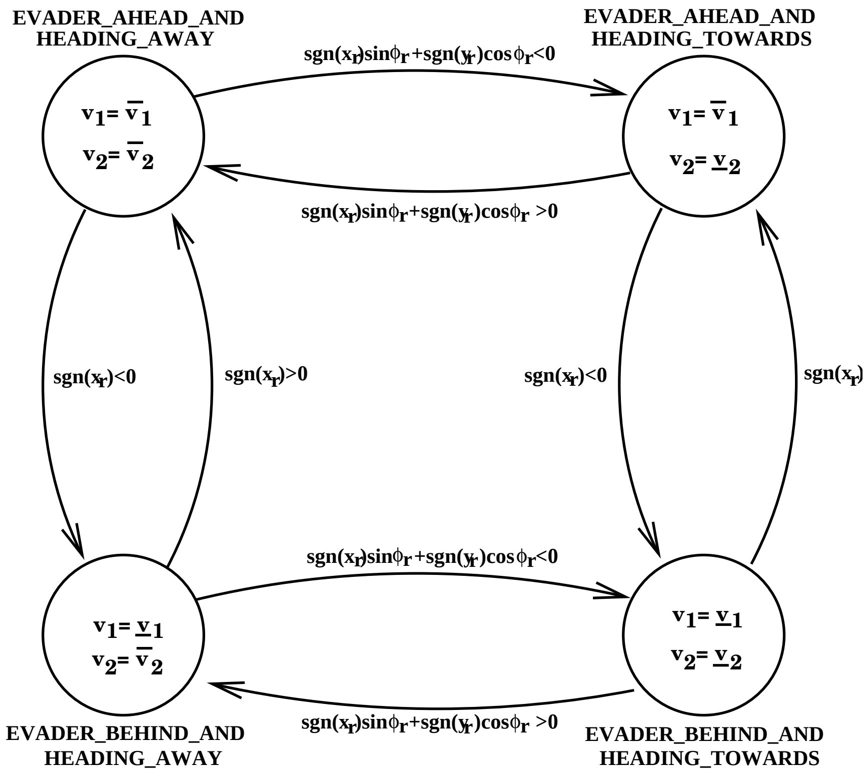

Figure 9: Abstraction of Saddle Solution as a Hybrid Automaton

Proposition 1 [Saddle Solution] *The global saddle solution* (u^*, d^*) *to the game described by system (27) for the cost* J *given by equation (22) is*

$$d^* = \begin{cases} \overline{v}_1 & \text{if } sgn(x_r) > 0 \\ \underline{v}_1 & \text{if } sgn(x_r) < 0 \end{cases} \tag{31}$$

$$u^* = \begin{cases} \overline{v}_2 & \text{if } sgn(x_r)\cos\phi_r + sgn(y_r)\sin\phi_r > 0 \\ \underline{v}_2 & \text{if } sgn(x_r)\cos\phi_r + sgn(y_r)\sin\phi_r < 0 \end{cases} \tag{32}$$

Proof: In [13]. □

As can be seen from equation (31), the worst disturbance depends on the position and orientation of the evader relative to the pursuer. If the evader is ahead of the pursuer then the pursuer should move as quickly as possible whereas if the evader is behind the pursuer then the pursuer should move as slowly as possible. Similarly, if the evader is heading towards the pursuer then the evader should move as slowly as possible, and if the evader is pointing away from the pursuer, the evader should move as quickly as possible. The bang-bang nature of the saddle solution allows us to abstract the system behavior by the hybrid automaton shown in Figure 9. This allows to express the saddle solution in a form of protocol. The automaton switches between four different discrete states and within each state, there exists a differential equation, namely equation (27) with v_0 and v_1 as shown in Figure 9.

The unsafe sets of states are illustrated in Figure 10 for various values of ϕ_r, and speed ranges as illustrated. Efficient storage and retrieval methods for safe sets in currently under investigation.

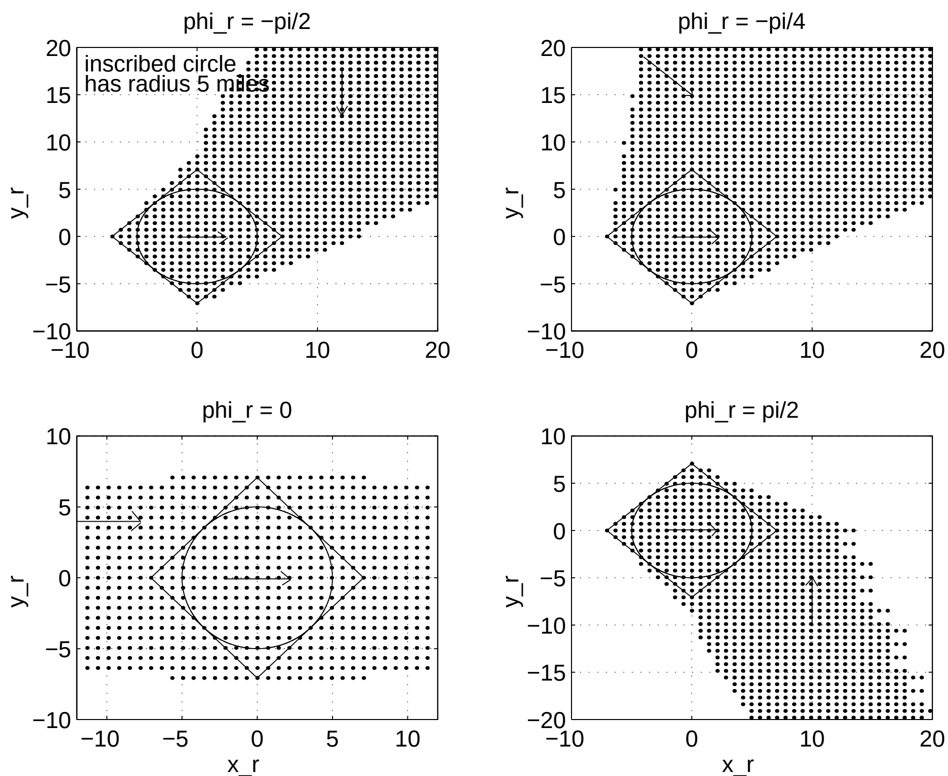

Figure 10: Unsafe sets $(x_r(0), y_r(0))$ for $[\underline{v}_1, \overline{v}_1] = [2, 4]$, $[\underline{v}_2, \overline{v}_2] = [1, 5]$ and $\phi_r = -\pi/2$, $-\pi/4$, 0, and $\pi/2$.

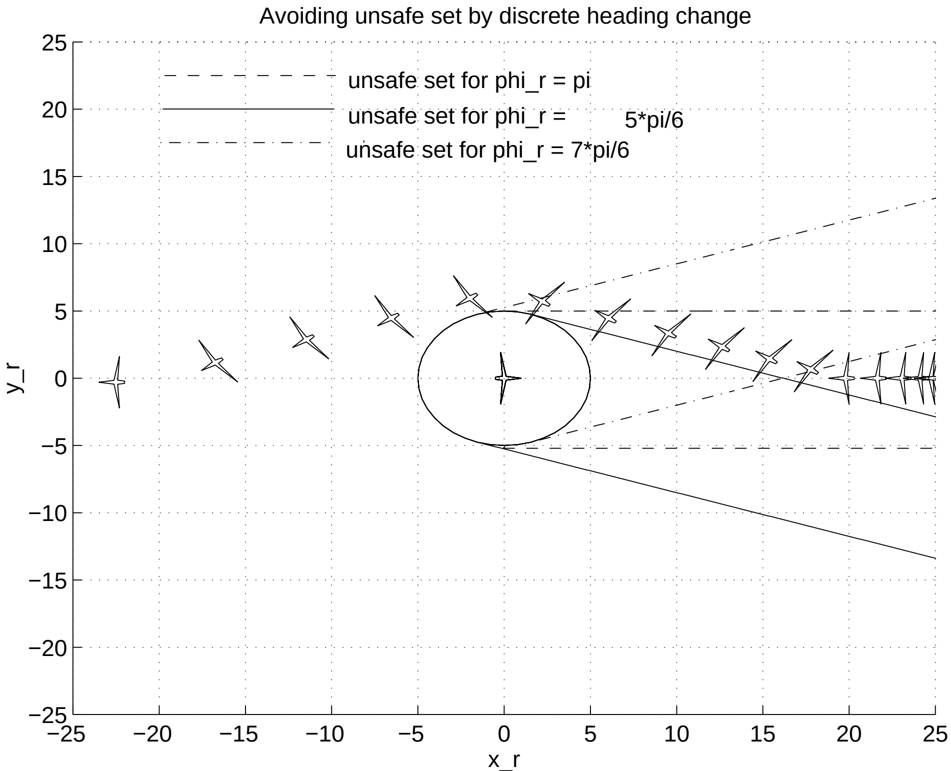

Figure 11: Showing a configuration which is initially unsafe, and the three discrete heading changes which avoid conflict and bring the aircraft back to course

4.2.2 Resolution by Discrete Heading Changes

Now consider case (ii), in which the evader can make discrete heading changes in order to resolve conflict. Such a scenario is displayed in Figure 11. The evader's configuration initially lies in the unsafe set of the pursuer, so the evader calculates the minimum heading change $\delta\phi_r$ in order to escape from the unsafe set. Referring to Figure 12, with

$$\begin{aligned} \alpha &= \tan^{-1}(\tfrac{y_r}{x_r}) \\ \beta &= \tan^{-1}(\tfrac{v_2 \sin \phi_r}{-v_1 + v_2 \cos \phi_r}) \\ \gamma &= \beta - \alpha \\ h &= \sqrt{x_r^2 + y_r^2} \\ d &= h \cos \gamma \end{aligned} \tag{33}$$

and r the radius of the target zone, then the coordinates of the point A may be calculated as

$$A = (r \sin \beta + d \cos \beta, d \sin \beta - r \cos \beta)$$

The heading change $\delta\phi_r$ is therefore calculated by determining the new value of ϕ_r required to make (x_r, y_r) coincide with A. This ensures that the evader's new position is outside the unsafe set, and that the evader moves tangent to this set until the zero range line is passed, at which point the evader may turn back to catch up with its original trajectory.

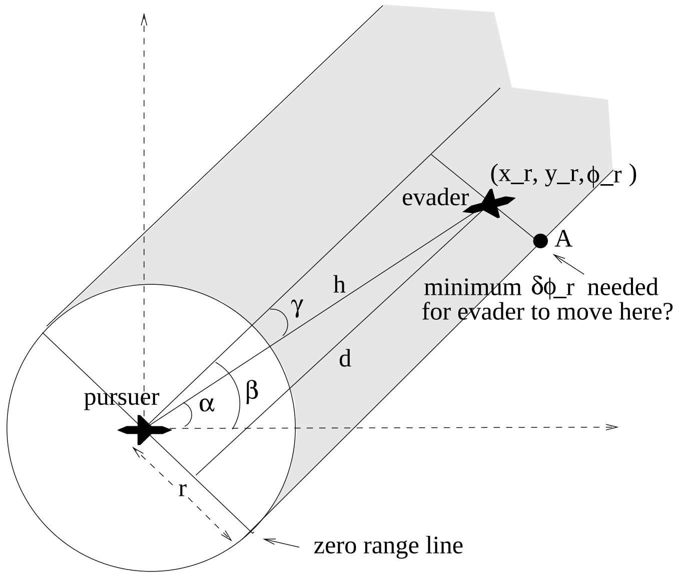

Figure 12: Calculating the minimum deviation angle $\delta\phi_r$ needed to get out of the unsafe set

5 Conclusions

In this paper, a conflict resolution strategy for use in Air Traffic Management Systems has been presented. Noncooperative conflict resolution methods were developed using game theory. Each aircraft treats potentially conflicting aircraft as players in a zero sum, noncooperative game and calculates an optimal policy for the worst possible actions of the other aircraft. Defending against the worst case scenario allows the aircraft to guarantee safety regardless of the actions of the other aircraft. Once the saddle solution to the game has been calculated, safe sets of initial conditions are computed by integrating backwards the Hamilton Jacobi equations. In addition, the class of safe controls can be also calculated by considering all control inputs which guarantee safety for the particular initial condition. Other objectives, such as efficiency or passenger comfort, can be accommodated in this framework by performing optimization over the class of safe controls.

The research presented in this paper needs to be extended in many directions. The safe set calculations must be numerically implemented for various types of aircraft encounters and must be efficiently stored in data bases in order to allow reliable and fast retrieval during flight.

Conflicts of more than two aircraft must also be considered. In addition, in some of these multi-aircraft conflicts, some of the player may be cooperating in resolving the conflict and some may not. This leads to a mixture of cooperative and noncooperative conflict resolution methods which can be formulated in the framework of group and team theory.

References

[1] RTCA Inc. Final Report of RTCA Task Force 3: Free Flight Implementation. Technical report, Washington, DC, October 1995.

[2] G.J. Couluris and S. Dorsky. Advanced air trasportation technologies (AATT) potential benefits analysis. Technical report, NASA Contract NAS2-13767, Seagull Technology, Inc., Cupertino, CA, September 1995.

[3] W.H. Harman. TCAS : A system for preventing midair collisions. *The Lincoln Laboratory Journal*, 2(3):437–457, 1989.

[4] Heinz Erzberger. CTAS : Computer intelligence for air traffic control in the terminal area. Technical report, NASA TM-103959, Ames Research Center, Moffett Field, CA, July 1992.

[5] L. Yang and J. Kuchar. Prototype conflict alerting logic for free flight. In *Proceedings of the 35th AIAA Aerospace Sciences Meeting & Exhibit*, Reno, NV, January 1997.

[6] R. A. Paielli and Heinz Erzberger. Conflict probability estimation for free flight. In *Proceedings of the 35th AIAA Aerospace Sciences Meeting & Exhibit*, Reno, NV, January 1997.

[7] J. Krozel, T. Mueller, and G. Hunter. Free flight conflict detection and resolution analysis. In *Proceedings of the AIAA Guidance, Navigation and Control Conference*, San Diego, CA, July 1996.

[8] J. Krozel and M. Peters. Conflict detection and resolution for free flight. *Air Traffic Control Quarterly Journal.* To apper in 1997.

[9] James Kuchar. Methodology for alerting-system performance evaluation. *Journal of Guidance, Control and Dynamics*, 19(2):438–444, 1996.

[10] Y. Nan and Y. Zhao. Terminal area synthesis and conflict resolution in the presence of inclement weather. Submitted to 36th IEEE Conference on Decision and Control, 1996.

[11] M. Shewchun and E. Feron. Linear matrix inequalities for analysis of free flight conflict problems. Submitted to 36th IEEE Conference on Decision and Control, 1996.

[12] V. Duong. Conflict resolution advisory for autonomous airborne separation in low density airspace. Submitted to 36th IEEE Conference on Decision and Control, 1996.

[13] C. Tomlin, G. Pappas, and S. Sastry. Conflict resolution for air traffic management systems: A case study in multi-agent hybrid systems. Technical Report UCB/ERL M96/38, University of California, Berkeley, 1996.

[14] S. Sastry, G. Meyer, C. Tomlin, J. Lygeros, D. Godbole, and G. Pappas. Hybrid control in air traffic management systems. In *Proceedings of the 1995 IEEE Conference in Decision and Control*, pages 1478–1483, New Orleans, LA, December 1995.

[15] C. Tomlin, G. Pappas, J. Lygeros, D. Godbole, and S. Sastry. A next generation architecture for air traffic management systems. Technical Report UCB/ERL M97/7, University of California, Berkeley, 1997.

[16] T. Başar and G. J. Olsder. *Dynamic Non-cooperative Game Theory.* Academic Press, second edition, 1995.

[17] Joseph Lewin. *Differential Games.* Springer Verlag, 1994.

[18] G. Owen. *Game Theory.* Academic Press, third edition, 1995.

[19] Héctor Sussmann. Shortest 3-dimensional paths with a prescribed curvature bound. In *Proceedings of the 1995 IEEE Conference in Decision and Control*, pages 3306–3312, New Orleans, LA, December 1995.

[20] L. E. Dubins. On curves of minimal length with a constraint on average curvature, and with prescribed initial and terminal positions and tangents. *Americal Journal of Mathematics*, 79:497–516, 1957.

[21] John Lygeros, Datta Godbole, and Shankar Sastry. A game theoretic approach to hybrid system design. Technical Report UCB/ERL M95/77, University of California, Berkeley, 1995.